Experimental Study On CFRP Strengthening And Concrete Overlays For Precast Concrete Slabs

Sayan Sirimontree[1], Charinrat Aiamlaoo[1], Amaras Mathuros[2], Min Jae Park[3], and Chanachai Thongchom[1*]

[1] *Thammasat University Research Unit in Structural and Foundation Engineering, Department of Civil Engineering, Thammasat School of Engineering, Thammasat University, Klongluang, Pathumthani 12120, Thailand.*
[2] *Department of Construction Engineering Technology, Faculty of Industrial Technology, Chiang Rai Rajabhat University, Chiang Rai 57100, Thailand.*
[3] *Department of Architectural Engineering, College of Engineering, Pukyong National University, Nam-gu, Busan 48513, Republic of Korea.*
[*] *Corresponding author. E-mail: tchanach@engr.tu.ac.th*

Received: Jul. 18, 2025; Accepted: Jan. 14, 2026

Precast concrete slabs are extensively used in construction, with Carbon Fiber Reinforced Polymer (CFRP) laminates effectively enhancing their structural performance. This study investigates the flexural performance of precast concrete slabs and overlays strengthened with CFRP laminates through four-point bending tests. Four specimens were tested, including one unreinforced slab and three CFRP-strengthened slabs with varying overlay configurations. The slabs measured 2500 mm in length, 350 mm in width, and 50 mm in thickness, and were strengthened with CFRP alone or combined with 50 mm and 100 mm concrete overlays. Results indicate that CFRP strengthening significantly enhanced structural performance, achieving a 195% increase in load-bearing capacity compared to unreinforced slabs, and 296% when combined with reinforced overlays. Increasing overlay thickness from 50 mm to 100 mm improved stiffness and reduced midspan deflection by 26%, albeit with a slight reduction in ductility. Reinforced overlays improved load capacity by 34% and ductility by 27% compared to regular overlays. These findings highlight the effectiveness of CFRP laminates and concrete overlays in optimizing the flexural performance of precast concrete slabs for high-performance structural applications.

Keywords: Precast concrete Slabs; CFRP; Concrete Overlays; Structural Performance; Strengthening

http://dx.doi.org/10.6180/jase.202608_31.062

1. Introduction

The growing demand for efficient and sustainable construction underscores the importance of enhancing structural performance in precast concrete systems. Precast concrete slabs and overlays are highly regarded for their construction efficiency, superior quality control, and cost-effectiveness. However, challenges such as aging materials, increased load demands, and evolving design standards require innovative strengthening techniques to maintain and improve structural integrity [1, 2]. Among these techniques, CFRP laminates stand out for their exceptional strength-to-weight ratio, corrosion resistance, and adaptability, making them ideal for enhancing flexural performance, ductility, and load-carrying capacity in precast and reinforced concrete (RC) structures [3–6].

Yee and Eng [7] demonstrated the economic and structural advantages of precast concrete, particularly in improving construction efficiency. Similarly, Al-Rousan et al. [8] This study further confirmed the effectiveness of

CFRP laminates in enhancing the load-bearing capacity and flexural performance of reinforced concrete elements. The results revealed that variations in CFRP configurations-such as unidirectional layouts, cross-ply arrangements, and multilayer applications-significantly influenced the overall structural behavior, particularly by increasing stiffness, delaying crack initiation, and controlling crack propagation. These findings demonstrate that CFRP strengthening is a highly efficient technique for mitigating material degradation and accommodating increased service loads, while simultaneously preserving the architectural aesthetics of both precast and cast-in-place concrete structures. Teng et al. [9] showed that applying CFRP laminates could increase the ultimate flexural strength of RC beams by approximately 25%, depending on material configurations and loading conditions. Similarly, Awoyera et al. [10] observed a 60.76% improvement in the ultimate load capacity of RC slabs retrofitted with CFRP laminates under controlled laboratory conditions, showcasing their potential to enhance flexural performance and reduce crack propagation. Azevedo et al. [11] further investigated fire-exposed RC slabs strengthened with near-surface mounted (NSM) CFRP laminates and concluded that effective fire protection measures could extend their performance to over 120 minutes under extreme conditions.

Naser et al. [12] and Ibrahim et al. [13] emphasized the critical role of CFRP laminates in enhancing structural stiffness and ductility, particularly under cyclic loading. Their studies highlighted the effectiveness of integrating CFRP with structural overlays to improve resistance against dynamic loads and reduce the risk of failure. These findings underscore the potential of CFRP systems in addressing both static and dynamic challenges in structural applications.

Achieving optimal performance through CFRP strengthening requires meticulous design and precise implementation. Mongkhonsang [14] demonstrated the utility of finite element analysis (FEA) in predicting stress redistribution and failure modes in CFRP-strengthened systems. Their findings highlight the critical role of accurate design and proper installation in ensuring the success of CFRP retrofitting, particularly in enhancing the flexural capacity and structural stability of RC elements under varied loading conditions. Additionally, Mohammadi et al. [15] and Amran et al. [16] emphasized the importance of thorough surface preparation, proper adhesive selection, and rigorous quality control to achieve a reliable bond between CFRP laminates and concrete substrates, maximizing the system's efficiency and durability.

Recent advancements in precast concrete systems have integrated innovative materials and techniques. The Precast Concrete Structures group [17] proposed strategies to optimize the performance of load-bearing precast elements strengthened with CFRP, while Siddika et al. [18] highlighted CFRP's role in mitigating material degradation in RC beams, extending the service life of precast elements.

CFRP systems have also demonstrated remarkable versatility in addressing modern construction challenges. May et al. [19] reported a 70% reduction in dead load with lightweight carbon-reinforced precast elements, improving structural efficiency. Derkowski and Surma [20] illustrated the benefits of integrating CFRP with structural toppings, which enhanced load distribution and composite action. Similarly, hybrid strengthening systems combining CFRP with sustainable materials, as explored by Awoyera et al. [10] and Swathy et al. [21], offer costeffective and environmentally friendly retrofitting approaches.

These findings underscore the need for tailored strengthening solutions that address diverse structural and site-specific requirements. While previous research has extensively validated the individual benefits of externally bonded CFRP systems for flexural strengthening and the use of concrete overlays for enhancing slab performance, limited attention has been devoted to the synergistic effects of combining these two techniques, particularly within the context of precast concrete slab systems. A significant knowledge gap remains regarding how specific variations in overlay properties, namely thickness and reinforcement detailing, influence the composite flexural behavior of CFRP-strengthened members. This study addresses this critical gap by systematically investigating the interplay between externally bonded CFRP laminates and diverse overlay configurations. Unlike prior studies, this research provides a direct experimental comparison of varying overlay thicknesses (50 mm vs. 100 mm) and reinforcement types (plain vs. reinforced). By doing so, it offers novel insights into optimizing the trade-off between strength, stiffness, and ductility, thereby providing practical guidelines for designing more efficient and resilient strengthening solutions.

2. Experimental program

2.1. Specimen design

This study fabricated four slab specimens to evaluate the flexural performance and load-bearing capacity of precast concrete slabs strengthened with CFRP sheets under four-point bending tests. The test setup included two wide-flange beams serving as supports, positioned 50 mm and 2450 mm from the slab edges. Two additional wide-flange beams were used to apply symmetrical loads around the

midspan, with load points located at 850 mm and 1650 mm from the edges. This configuration accurately simulated bending behavior and allowed consistent application of loads until failure.

The slabs, measuring 2500 mm in length, 350 mm in width, and 50 mm in thickness, were produced in a controlled factory environment to ensure precision and uniformity. All specimens underwent a curing process of at least 28 days to achieve optimal compressive strength. The specimens were prestressed with high-strength steel wires to enhance their structural performance. External strengthening was applied using externally bonded CFRP sheets (EBCFRP sheets), which were strategically placed 200 mm from the support points on both sides to maximize their effectiveness in flexural reinforcement.

For specimens with concrete overlays, variations in overlay thickness (50 mm and 100 mm) and reinforcement type were incorporated to evaluate their effects on flexural performance. Reinforced concrete overlays (RC10) were included to provide insights into the comparative behavior of plain and reinforced overlays. These variations were critical for understanding the interaction between the overlay material, CFRP sheets, and the precast slab core under applied loads.

The specimen labels were defined based on their configurations to distinguish the variations in design. PC refers to precast slabs without overlays, serving as the control group. PC-C5 represents slabs with a 50 mm concrete overlay, while PC-C10 refers to slabs with a 100 mm concrete overlay. PC-RC10 denotes slabs with a 100 mm reinforced concrete overlay. These labels facilitate clear identification of each specimen and their specific configurations.

The detailed specifications and properties of the slabs are summarized in Table 1.

This design enabled a comprehensive evaluation of the flexural performance and loadbearing capacity of precast concrete slabs, particularly with CFRP sheet strengthening. The variations in overlay thickness and type provided valuable insights into the interactions among slab components under load. The experimental framework, including the test setup and specimen configurations, is illustrated in Figure 1 and Figure 2, which highlight the structural details and loading arrangement used in the study.

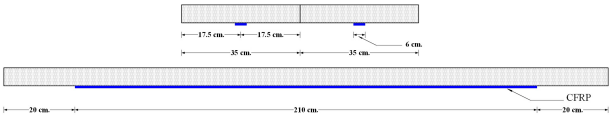

Fig. 1. Schematic representation of specimen strengthening with CFRP sheets showing longitudinal profile and reinforcement details.

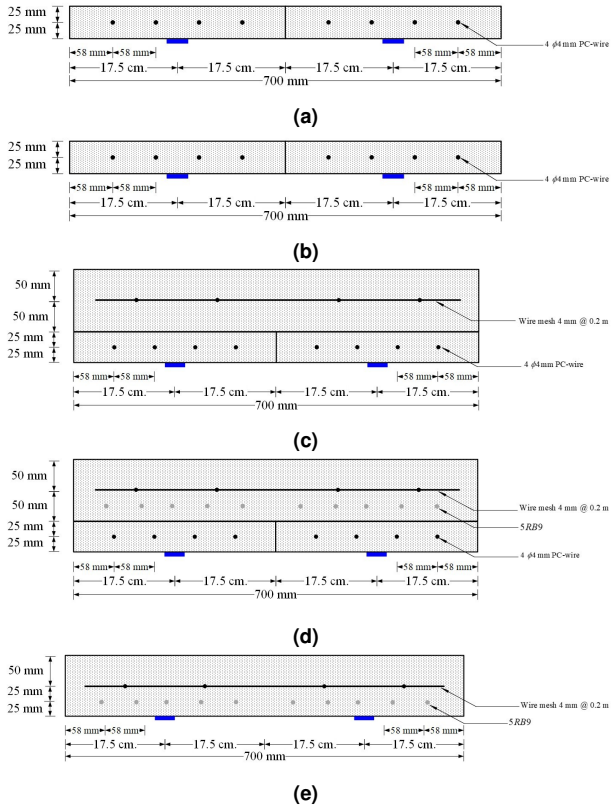

Fig. 2. Detailed cross-sectional configurations of the tested slabs: (a) Control slab PC; (b) Slab with 50 mm overlay PC-C5; (c) Slab with 100 mm overlay PC-C10; (d) Slab with reinforced 100 mm overlay PC-RC10.

2.2. Materials

The materials utilized in this study were meticulously selected and prepared to ensure compatibility and reliability in achieving the desired structural performance. All materials adhered to relevant international standards, ensuring consistency and accuracy in the experimental results. Four precast concrete slab specimens were fabricated in a controlled environment to guarantee precise dimensions and uniform material properties. The slabs were cured for at least 28 days to achieve the required mechanical properties. Detailed material properties and associated standards are presented below.

2.2.1. Concrete

The precast concrete slabs were fabricated using a custom mix designed to meet structural performance requirements. For specimens with concrete overlays, the mix was optimized for improved workability and compatibility with the existing slab surface. The concrete achieved a minimum

Table 1. Experimental specifications of the slabs.

Specimen	Type of slab	Thickness slab (mm)	Type of concrete overlay	Thickness concrete overlay (mm)	Type of strengthening method
PC	Precast	50	-	-	EB-CFRP sheets
PC-C5	Precast	50	Concrete overlay	50	EB-CFRP sheets
PC-C10	Precast	50	Concrete overlay	100	EB-CFRP sheets
PC-RC10	Precast	50	Reinforced concrete	100	EB-CFRP sheets

compressive strength of 28 MPa after 28 days of curing, as verified according to ASTM C39 [22].

2.2.2. High-strength steel wires

Prestressing was achieved using high-strength steel wires conforming to ASTM A421 [23], ensuring superior load-bearing capacity and minimized deflection under service loads. The high-strength steel wires used in this study had a diameter of 4 mm and a cross-sectional area of 12.57 mm^2. These wires exhibited a tensile strength of $1,715$MPa.

2.2.3. Reinforcement in concrete overlay

The concrete overlays were reinforced using wire mesh and plain round steel bars to enhance stress distribution, crack control, and ductility. Wire mesh reinforcement adhered to ASTM A185 [24], while steel bars conformed to ASTM A615 [25]. The wire mesh reinforcement used in the concrete overlays had a diameter of 4 mm and a cross-sectional area of 12.57 mm^2. It demonstrated a yielding strength of 540 MPa , contributing to enhanced stress distribution, crack control, and overall ductility. The plain round steel bars used for reinforcement had a diameter of 9 mm and a cross-sectional area of 63.6 mm^2. These bars possessed an elastic modulus of 210 GPa , with a yielding strength of 235 MPa and a tensile strength of 385 MPa , ensuring effective load transfer and resistance to cracking.

2.2.4. CFRP sheets

The externally bonded CFRP sheets applied for strengthening had a width of 50 mm and a thickness of 0.12 mm . These sheets provided a tensile strength of $3,100$MPa, significantly improving the tensile capacity and structural performance of the precast concrete slabs. These sheets complied with ASTM A370 [26].

2.2.5. Epoxy adhesive

The epoxy adhesive used for bonding the CFRP sheets had an elastic modulus of 11.2 GPa and a tensile strength of 29 MPa . This adhesive played a crucial role in ensuring effective load transfer between the CFRP sheets and the concrete substrate, contributing to the overall durability and efficiency of the strengthening system.

2.3. Strengthening process

The strengthening process follows systematic steps to ensure effective bonding of CFRP sheets to the concrete surface, as illustrated in Figure 3. The figure highlights key stages: surface preparation with a diamond grinder for a smooth finish, uniform application of epoxy adhesive, and precise placement of CFRP sheets aligned with the designated reinforcement spacing. These steps are essential to achieving optimal adhesion and reinforcement effectiveness, which directly impact structural performance under loading.

The concrete surface is ground with a diamond grinder to remove irregularities and achieve a smooth finish. This step eliminates potential weak points, such as sharp edges or contaminants that could impair bonding. A moisture meter is used to ensure the surface is sufficiently dry before proceeding to the next stage. Dust and debris generated during grinding are removed using compressed air and brushes, leaving a clean bonding surface.

After surface preparation, the CFRP sheets are cut to specified lengths based on design requirements. An epoxy adhesive, formulated for high bond strength and durability, is applied uniformly across the prepared area. Ensuring even adhesive coverage prevents weak spots that could lead to delamination or reduced reinforcement efficacy. The CFRP sheets are then carefully placed onto the adhesive-coated surface, aligned precisely with the designated reinforcement spacing. Precision at this step ensures effective load distribution and optimal structural performance [14].

For each precast slab, a single layer of CFRP sheet is applied to reinforce critical regions, including the midspan and areas near the support points. This configuration enhances flexural and shear capacity, effectively addressing potential failure modes and optimizing slab performance under bending loads.

Once the CFRP sheets are installed, the specimens undergo a curing period of at least two weeks. This curing process allows the epoxy adhesive to reach full strength, ensuring a robust bond between the CFRP sheets and the concrete. Proper curing is critical for the long-term durabil-

ity and reliability of the strengthened specimens.

This comprehensive strengthening process ensures consistent CFRP application and maximizes performance under testing conditions. By adhering to these precise steps, the study achieves reproducible results and provides valuable insights into the use of CFRP for structural reinforcement.

Fig. 3. Procedure of the strengthening method.

Surface preparation: The concrete surface is ground with a diamond grinder to achieve a smooth, even finish and ensure optimal adhesion.

Epoxy application: An epoxy adhesive is uniformly applied to bond the CFRP sheets to the concrete. It is carefully spread over the designated areas to en sure consistent coverage.

CFRP placement: The CFRP sheets are placed with precision, aligned to the designed reinforcement spacing to ensure accuracy and adherence to the structural design.

2.4. Test setup

The experimental setup for the four-point bending test, as shown in Figure 4, was systematically designed to evaluate the flexural performance of precast concrete slabs. The test setup utilized two wide-flange beams functioning as support points and two additional wideflange beams for load application.

The support points were located at 50 mm and 2450 mm from the specimen edges, creating a clear span of 2400 mm Load points were symmetrically positioned at 850 mm and 1650 mm from the edges to ensure a uniform bending moment within the midspan. This configuration effectively replicated realistic structural loading conditions, allowing for a focused evaluation of the specimens' flexural behavior.

A load cell was used to measure the applied force on the specimens with high precision. To monitor deflection, a Linear Variable Differential Transformer (LVDT) was installed at the midspan of each slab. This instrumentation provided accurate measurements of both the applied load and the corresponding deflection, which are critical parameters for evaluating structural performance.

The load was applied incrementally using a hydraulic loading system. For most specimens, the load was applied at a rate of 1 ton per minute, ensuring a consistent and controlled testing process. However, the first specimen was subjected to a slower loading rate of 0.2 tons per minute to observe its initial behavior and ensure system stability. Loading continued until failure, providing comprehensive data on the load-bearing capacity and failure modes of the slabs.

The applied load and midspan deflection were recorded in real-time using a data acquisition system, enabling both live monitoring and detailed post-test analysis. The collected data was processed to generate load-deflection curves, which illustrate the relationship between applied load and deflection. These curves highlight key metrics such as stiffness, cracking load, and ultimate capacity.

The systematic design of the test setup ensured consistency across all specimens, enabling accurate comparisons of their structural behavior under similar loading conditions. The results obtained from this setup significantly contribute to understanding the impact of different strengthening configurations on the flexural performance of precast concrete slabs.

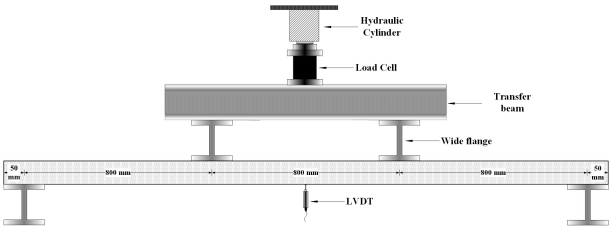

Fig. 4. Experimental setup for structural testing.

3. Results and discussions

3.1. Overall responses

3.1.1. Load and deflection

The load and deflection behavior of the four slab specimens tested in this study is summarized in Table 2 and illustrated in Figure 5. Key parameters such as cracking load (Pcr), yield load (Pyield), and maximum load (Pmax) were recorded along with their corresponding deflections (Δ Pcr, Δ Pyield, and Δ Pmax). The specimens were subjected to four-point bending tests, and the results provide insight into the influence of concrete overlay and reinforcement with CFRP sheets. Among the specimens, PC-RC10 exhibited the highest load-carrying capacity, followed by PC-C10, PC-C5, and PC. These results highlight the significant role of concrete overlays and reinforcement configurations in enhancing the load-bearing capacity and stiffness of precast concrete slabs.

The specimen with reinforced concrete overlay (PC-RC10) exhibited a maximum load 34% higher than those with regular concrete overlays of both 50 mm and 100 mm thickness. In comparison, the specimen without an overlay (PC) demonstrated a maximum load 75% lower than PC-RC10, emphasizing the importance of overlays in enhancing structural performance.

In terms of deflection, PC-RC10 showed 333% less deformation at maximum load compared to the specimen without an overlay (PC), underscoring its higher stiffness. The difference in deflection between specimens with 50 mm and 100 mm overlays was 26%, with the thicker overlay offering greater stiffness. However, the improvement in stiffness for the 100 mm overlay compared to the reinforced overlay was marginal, with only a 1% difference.

Ductility, as reflected by the ductility ratio, varied significantly among the specimens. The specimen with the 50 mm overlay (PC-C5) exhibited a ductility ratio 27% higher than the reinforced overlay (PC-RC10), but the specimen without an overlay (PC) demonstrated a ductility ratio 68% lower than PC-RC10, indicating brittle behavior. These results confirm that reinforced overlays effectively balance strength, stiffness, and deformation capacity.

3.1.2. Section analysis for composite slabs

The section analysis for composite slabs, illustrated in Figure 6, evaluates their structural performance under flexural loading in detail. The analysis considers the contributions of prestressing steel, cast-in-situ reinforcement, precast reinforcement, and EB-CFRP sheets. These materials form a composite system comprising a precast concrete slab, an in-situ concrete layer, and CFRP sheets on the tension face. The study focuses on understanding the strain and stress

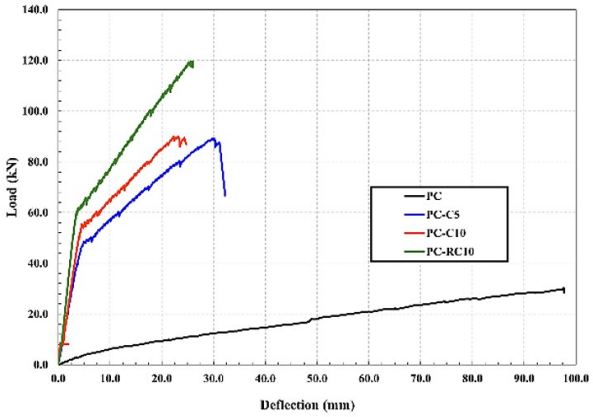

(a) Load-deflection relationship.

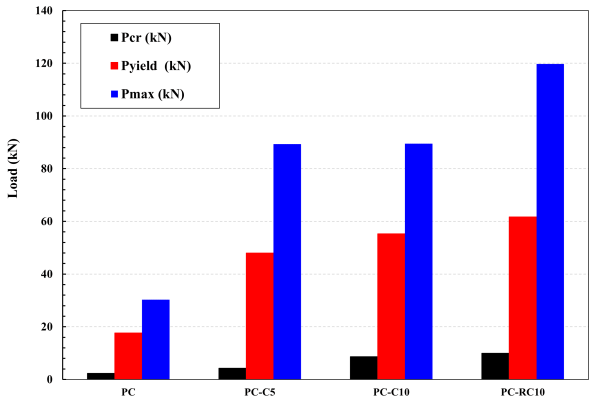

(b) Critical load parameters: Cracking load (P_{cr}), Yield load (P_{yield}), and Maximum load (P_{max}).

Fig. 5. Load-deflection behavior and key load parameters.

distribution, calculating forces in individual components, and determining the moment and ultimate load capacity, ensuring the structural integrity and optimization of the slab.

The strain distribution in Figure 6b follows the principle of plane sections remaining plane after bending, resulting in a linear strain gradient. The neutral axis divides the section into compression and tension zones, with the upper region of the concrete under compression and the reinforcement layers below experiencing tension. The height of the compression block (a) is calculated using $a = \beta_1 \cdot c$, where β_1 is a factor reflecting the concrete's stress distribution, and c is the depth to the neutral axis. This calculation ensures an accurate determination of the concrete's effective contribution to resisting flexural forces. The stress distribution in Figure 6c mirrors the strain profile, with compression in the upper region and tension in the reinforcement and CFRP layers, maintaining balanced force equilibrium

Table 2. Experimental results.

Specimen	P_{cr} (kN)	P_{yield} (kN)	$P_{\max}$ (kN)	ΔP_{cr} (mm)	ΔP_{yield} (mm)	$\Delta P_{\max}$ (mm)	$\Delta P_{\max}/\Delta P_{\text{yield}}$ (mm)
PC	2.3	17.7	30.3	3.17	48.9	97.7	2.0
PC-C5	4.3	48.0	89.3	0.42	3.8	30.1	7.9
PC-C10	8.7	55.3	89.5	0.43	4.6	22.3	4.9
PC-RC10	10.0	61.7	119.7	0.72	3.6	22.6	6.2

across the section.

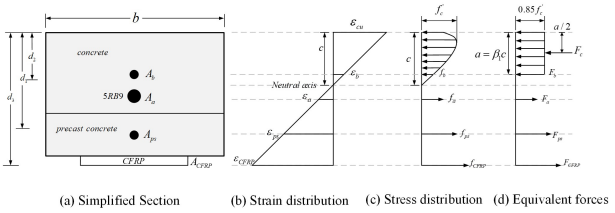

Fig. 6. Cross-sectional analysis of the composite slab.

The moment capacity (M_n) of the composite section integrates the contributions from all materials and is expressed as:

$$M_n = F_{ps} \cdot \left(d_1 - \frac{a}{2}\right) + F_a \cdot \left(d_2 - \frac{a}{2}\right) + F_b \cdot \left(d_2 - \frac{a}{2}\right) + F_{CFRP} \cdot \left(d_3 - \frac{a}{2}\right) \quad \text{(Eq.1)}$$

Where d_1, d_2, and d_3 represent the effective depths of the prestressing steel, reinforcement, and CFRP, respectively; a denotes the depth of the compression block; and F_{ps}, F_a, F_b, and F_{CFRP} correspond to the forces in their respective layers. These variables are crucial for calculating the composite section's flexural capacity, ensuring that the contributions from all materials are accurately represented.

The forces in individual materials are determined based on their respective stress-strain relationships. For prestressing steel, the force is computed as:

$$F_{ps} = \begin{cases} E_{ps}\varepsilon_{ps}A_{ps} & ;\varepsilon_{ps} < \varepsilon_{yps} \\ f_{yps}A_{ps} & ;\varepsilon_{ps} \geq \varepsilon_{yps} \end{cases} \quad \text{(Eq.1a)}$$

Similarly, the forces in cast-in-situ reinforcement (F_a) and precast reinforcement (F_b) are given by:

$$F_a = \begin{cases} E_a\varepsilon_a A_a & ;\varepsilon_a < \varepsilon_{ya} \\ f_{ya}A_a & ;\varepsilon_a \geq \varepsilon_{ya} \end{cases} \quad \text{(Eq.1b)}$$

$$F_b = \begin{cases} E_b\varepsilon_b A_b & ;\varepsilon_b < \varepsilon_{yb} \\ f_{yb}A_b & ;\varepsilon_b \geq \varepsilon_{yb} \end{cases} \quad \text{(Eq.1c)}$$

The CFRP layer, unlike steel, does not yield but fails upon reaching its ultimate tensile strength. The force in the CFRP is calculated as:

$$F_{CFRP} = \begin{cases} E_{CFRP}\varepsilon_{CFRP}A_{CFRP} & ;\varepsilon_{CFRP} < \varepsilon_{uCFRP} \\ f_{uCFRP}A_{CFRP} & ;\varepsilon_{CFRP} \geq \varepsilon_{uCFRP} \end{cases} \quad \text{(Eq.1d)}$$

Where E_{ps}, E_a, E_b, and E_{CFRP} are the moduli of elasticity for the prestressing steel, cast-insitu reinforcement, precast reinforcement, and CFRP, respectively; $\varepsilon_{ps}, \varepsilon_a, \varepsilon_b$, and ε_{CFRP} are the strains in these materials; and f_{yps}, f_{ya}, f_{yb}, and f_{uCFRP} are the yield strengths or ultimate tensile strengths. These equations provide accurate force calculations under varying loading conditions.

The ultimate load capacity of the composite slab is calculated from the moment capacity using the formula:

$$\text{Load} = M_n \times \frac{6}{L} \times 2 \quad \text{(Eq.2)}$$

Where M_n is the moment capacity of the section; L is the span length of the slab; the term $6/L$ represents the relationship between moment and load in continuous slabs; and the multiplier 2 accounts for both positive and negative bending moments. This formula provides a robust framework for estimating the slab's load-carrying capacity under symmetrical loading.

To validate the accuracy of the proposed analytical formulations, the ultimate loadcarrying capacities calculated using Eq.1 and Eq.2, denoted as $\boldsymbol{P}_{\text{ana}}$, were compared with the experimental maximum loads ($\boldsymbol{P}_{\text{exp}}$). The material properties used in the calculation were based on the actual tested strengths: $f_{pu} = 1{,}715$MPa for prestressing wires, $f_{fu} = 3{,}100$MPa for CFRP, and the yield strength of RB9 bars in the overlay. The comparison results are summarized in Table 3.

Table 3. Comparison between experimental and analytical ultimate loads.

Specimen	P_{exp} (kN)	P_{ana} (kN)	Ratio ($P_{\text{exp}}/P_{\text{ana}}$)
PC	30.3	15.2	1.99
PC-C5	89.3	48.0	1.86
PC-C10	89.5	89.0	1.01
PC-RC10	119.7	118.5	1.01
Mean			1.47
SD			0.53

The ratio of experimental to analytical values (

P_{exp} / P_{ana}) serves as an indicator of the model's accuracy. As shown in the table, the analytical predictions for the thicker composite slabs are in excellent agreement with the experimental results. Specifically, the ratio for both PC-C10 and PC-RC10 is 1.01 , demonstrating the model's capability to accurately capture the composite flexural behavior.

For the thinner slabs (PC and PC-C5), the model provides a conservative prediction with ratios of 1.99 and 1.86, respectively. This apparent discrepancy is attributed to arching action (or compressive membrane action). The thinner slabs experienced significant deflection (up to 97.7 mm for PC) prior to failure. This large deformation, combined with the friction and restraint at the supports, allows the formation of a compressive strut mechanism that enhances load-carrying capacity beyond the pure flexural strength predicted by section analysis. Consequently, the proposed analytical method is confirmed to be effective and safe for estimating the structural capacity of CFRP-strengthened precast slabs.

3.1.3. Failure mode

The failure modes observed in the experiments provided critical insights into the structural behavior and limit states of the CFRP-strengthened specimens. For all slabs strengthened with CFRP (PC, PC-C5, PC-C10, and PC-RC10), the governing failure mode was the premature debonding of the CFRP laminate from the concrete substrate. This debonding occurred prior to the tensile rupture of the CFRP composite material, indicating that the ultimate tensile strain of the CFRP fibers was not reached during the tests. The failure process typically initiated with the formation of flexural cracks in the concrete slab within the constant moment region. As these cracks widened under increasing load, they induced high interfacial shear and normal stress concentrations at the bond line between the concrete and the CFRP laminate. This phenomenon, known as Intermediate Crack (IC) debonding, propagated towards the supports, leading to the complete separation of the laminate as shown in Figure 7a.

A detailed post-failure inspection of the fracture surfaces revealed a mixed-mode failure mechanism at the interface. In certain regions, the failure occurred at the concrete-adhesive interface, characterized by a separation of the epoxy layer from the concrete substrate, leaving the concrete surface relatively clean. Simultaneously, distinct areas exhibited cohesive failure within the concrete substrate. This was evidenced by a thin layer of concrete aggregate and mortar remaining attached to the debonded CFRP strip, as illustrated in the close-up view in Figure 7b. The corresponding rough texture of the concrete surface (Figure 7c) confirms that in these locations, the bond strength of the epoxy adhesive exceeded the tensile strength of the concrete surface layer.

(a) Overall view of CFRP delamination initiated by flexural cracks.

(b) Close-up of a debonded CFRP strip showing attached concrete fragments, indicating cohesive failure within the substrate.

(c) The corresponding rough concrete surface texture after debonding, confirming the mixed-mode nature of the interfacial failure.

Fig. 7. Predominant failure modes observed in CFRP-strengthened specimens.

Crucially, no cohesive failure was observed within the adhesive layer itself, confirming that the epoxy was properly mixed and cured. The dominance of bond-related failure modes underscores that the interfacial bond strength, rather than the tensile capacity of the CFRP material, is the limiting factor governing the ultimate load-carrying capacity of these strengthened precast slabs.

3.2. Effect of parameters

The results of this study highlight the significant influence of overlay thickness, overlay type, and strengthening method on the structural performance of CFRP-strengthened precast concrete slabs. Increasing the thickness of the concrete overlay improves stiffness and reduces deflection, though it has diminishing effects on load capacity and a notable trade-off with ductility. Reinforced concrete overlays consistently outperform regular overlays, demonstrating superior load-carrying capacity, energy absorption, and ductility. Additionally, the combination of CFRP with reinforced overlays provides the most effective strengthening solution, achieving up to a 296% increase in load-carrying capacity compared to unstrengthened slabs. These findings corroborate prior studies [27, 28], confirming that optimizing these parameters is essential for enhancing the structural performance of precast concrete slabs in various applications.

The findings from prior studies strongly align with the current research in emphasizing the benefits of combining CFRP and concrete overlays to enhance structural performance. For example, Hoang et al. [27] demonstrated that integrating ultra-high-performance concrete (UHPC) in the compression zone with CFRP in the tension zone significantly improved flexural capacity by up to 40%, while reducing deflection by $1.9 - 2.3$ times. These results validate the current study's observation that the combination of CFRP and reinforced overlays achieves up to a 296% increase in load-carrying capacity. Similarly, El-taly et al. [28] highlighted that CFRP strips effectively enhanced load-bearing capacity and ductility under negative bending moments, supporting the ductility improvements observed in this study. Together, these consistent findings confirm the critical role of CFRP and reinforced overlays in optimizing the structural performance of precast concrete slabs.

3.2.1. *Thickness of concrete overlay*

Overlay thickness significantly impacts structural behavior. Increasing the overlay thickness from 50 mm to 100 mm improved load-carrying capacity by less than 1% but reduced deflection by 26%. This highlights the diminishing returns in strength improvement with increased thickness, while stiffness showed a noticeable enhancement. However, the ductility ratio decreased by 38%, indicating a trade-off between stiffness and deformation capacity.

While increasing the overlay thickness from 50 mm to 100 mm yielded a significant 26% reduction in midspan deflection, demonstrating a marked improvement in serviceability, this enhancement was accompanied by a notable 38% decrease in the ductility ratio. This inverse relationship between stiffness and ductility is a critical finding that warrants a deeper discussion, as it carries significant implications for structural design and safety. The mechanism driving this trade-off is rooted in the alteration of the section's flexural behavior. The addition of a thick concrete overlay substantially increases the flexural rigidity (EI) and shifts the neutral axis upwards, thereby enlarging the compression zone depth. Consequently, under ultimate loading conditions, the extreme compression fiber of the concrete may reach its ultimate compressive strain limit ($\varepsilon_{cu} = 0.003$) and initiate crushing before the tensile reinforcement (both the internal steel and external CFRP) undergoes extensive yielding. This phenomenon represents a shift towards a compression-controlled failure mode, characteristic of a more brittle structural response where failure is governed by sudden concrete crushing rather than ductile steel yielding.

From a design perspective, this finding underscores a crucial optimization challenge. While increased stiffness is highly beneficial for satisfying serviceability limit states (SLS), such as controlling deflections and vibrations, a significant reduction in ductility can compromise structural safety at the ultimate limit state (ULS), particularly in seismic-prone regions. Ductility is fundamental to a structure's capacity to dissipate energy through inelastic deformation. Recognizing this, design guidelines such as ACI 440.2R [29] ("Guide for the Design and Construction of Externally Bonded FRP Systems for Strengthening Concrete Structures") impose strict limits on the strengthening ratio and apply strength reduction factors to prevent overly brittle, compression-controlled failures. Therefore, when designing thick overlays with CFRP, engineers must carefully balance the enhancement of stiffness with the preservation of adequate ductility to ensure the retrofitted structure remains both robust and resilient.

3.2.2. *Type of concrete overlay*

The type of concrete overlay plays a vital role in structural performance. Reinforced concrete overlays improved maximum load capacity by 34% compared to regular overlays of the same thickness and enhanced the ductility ratio by 27%. This demonstrates the superior energy absorption and load transfer efficiency of reinforced overlays, which make them more suitable for high-performance applications.

3.2.3. Strengthening method

The strengthening method also significantly influences structural performance. Specimens strengthened solely with CFRP exhibited significantly lower load-carrying capacity and stiffness. The addition of a 50 mm overlay increased maximum load by 195% and reduced deflection by 69%. Increasing the overlay thickness to 100 mm further reduced deflection by 26%, with minimal improvement in load capacity. Reinforced overlays combined with CFRP resulted in a maximum load 296% higher than specimens without overlays and provided an optimal balance between strength, stiffness, and ductility.

3.2.4. Synergistic Interaction between Concrete Overlays and CFRP Strengthening

The remarkable improvement in load-carrying capacity, particularly the 296% increase observed in specimen PC-RC10 compared to the unstrengthened slab, is attributed to a powerful synergistic interaction between the concrete overlay and the CFRP laminate. This enhancement is not merely additive but results from the combination of several critical structural mechanisms. Primarily, the addition of the concrete overlay significantly increases the overall depth of the composite section. This geometric alteration shifts the neutral axis upwards, thereby substantially increasing the internal lever arm-the vertical distance between the resultant compressive force in the overlay and the resultant tensile force in the CFRP and steel reinforcement. Since moment capacity is directly proportional to the lever arm, this enhanced composite action leads to a multiplicative increase in the slab's ultimate flexural capacity.

Furthermore, to fully utilize the high tensile strength of CFRP, the member must possess a compression zone robust enough to maintain force equilibrium. In thin precast slabs, premature failure often occurs due to concrete crushing before the CFRP can reach its ultimate capacity. The concrete overlay provides an enlarged and substantial compression zone, effectively resisting the induced compressive stresses. This prevents premature crushing and allows for the full mobilization of the CFRP's high tensile capacity, enabling the system to sustain significantly higher ultimate loads. Additionally, the increased stiffness provided by the thick overlay reduces the curvature of the slab under a given load. This reduced curvature promotes a more uniform distribution of interfacial shear and normal stresses along the bond line, particularly minimizing stress concentrations at the CFRP plate ends where peeling typically initiates. By delaying the onset of debonding, the overlay allows the composite section to deform further and carry higher loads.

Finally, the inclusion of steel reinforcement within the overlay (as in PC-RC10) plays a vital role in maintaining structural integrity. This reinforcement controls crack propagation and provides confinement within the topping concrete, ensuring the integrity of the compression zone and facilitating effective stress redistribution across the slab width. This mechanism explains the superior ductility and strength of the reinforced overlay compared to the plain concrete overlay, as it prevents localized stress concentrations that could otherwise lead to premature failure.

4. Conclusions

This study investigated the flexural performance of precast concrete slabs strengthened with externally bonded CFRP laminates and varying concrete overlay configurations. Based on the experimental results, the following key conclusions and practical implications are drawn:

- Composite Strengthening Efficiency: The integration of CFRP laminates with concrete overlays proved to be a highly effective retrofitting strategy. This composite system achieved a load-bearing capacity increase of up to 195% compared to slabs strengthened with CFRP alone, demonstrating significant synergistic benefits.
- Trade-off between Stiffness and Ductility: Increasing the overlay thickness from 50 mm to 100 mm significantly enhanced stiffness, reducing midspan deflection by 26%. However, this improvement resulted in a 38% reduction in the ductility ratio. This finding highlights a critical design trade-off where increased stiffness may lead to a more brittle, compression-controlled failure mode.
- Superiority of Reinforced Overlays: Reinforced concrete overlays exhibited superior structural performance compared to plain overlays of equivalent thickness. The inclusion of reinforcement increased the ultimate load capacity by 34% and improved the ductility ratio by 27%, ensuring better energy absorption and structural resilience.
- Optimal Configuration: The most effective strengthening solution evaluated was the combination of CFRP laminates with a reinforced concrete overlay (PC-RC10). This configuration yielded the highest load-bearing capacity, representing a 296% increase over the control slab, while maintaining a balanced ductility ratio. This characteristic makes it ideal for high-performance structural applications.

Practical Implications: For practical retrofitting, engineers should prioritize the use of reinforced overlays in

conjunction with CFRP to maximize both capacity and ductility. While thicker overlays offer superior stiffness control for serviceability, the potential reduction in ductility must be carefully managed in the design process to prevent brittle failure.

Limitations and future research

This study provides valuable preliminary insights into the flexural strengthening of precast slabs; however, the experimental program was limited to a single specimen per configuration. Consequently, the statistical significance of the findings is constrained, and the results should be viewed as indicative of performance trends rather than definitive design values. To establish statistical reliability, future research should prioritize testing a larger sample size with replicate specimens to validate the consistency of the observed behaviors and failure modes. Subsequent studies should also expand the experimental matrix to investigate additional parameters, such as the effect of multiple CFRP layers and alternative anchorage systems. Furthermore, comprehensive instrumentation, including strain gauges along the CFRP laminates, is recommended to quantitatively capture the strain distribution and interfacial stress transfer, providing essential data for refining and validating analytical models.

Acknowledgments

This research is supported by Thailand Science Research and Innovation (TSRI) Fundamental Fund, fiscal year 2026. And, the authors would like to acknowledge Retrofit Structure Specialist Co., Ltd. for providing composite materials and strengthening the specimens. This research received no specific grant from any funding agency in the public, commercial, or not-for-profit sectors. The Authors declares that there is no conflict of interest.

References

[1] R. L'Hermite, (1977) *"Use of bonding techniques for reinforcing concrete and masonry structures"* **Matériaux et Construction *10***(2): 85–89. DOI: https://doi.org/10.1007/BF02474856.

[2] Z. Ouyang and B. Wan, (2009) *"An analytical model of FRP-concrete bond deterioration in moist environment"* **Advances in Structural Engineering *12***(6): 761–769. DOI: https://doi.org/10.1260/136943309790327680.

[3] M. Shahawy, M. Arockiasamy, T. Beitelman, and R. Sowrirajan, (1996) *"Reinforced concrete rectangular beams strengthened with CFRP laminates"* **Composites Part B: Engineering *27***(3-4): 225–233. DOI: https://doi.org/10.1016/1359-8368(95)00044-5.

[4] W. Xue, Y. Tan, and L. Zeng, (2008) *"Experimental studies of concrete beams strengthened with prestressed CFRP laminates."* **PCI journal *53***(5): DOI: https://doi.org/10.15554/pcij.09012008.70.85.

[5] C. A. Neagoe. *"Concrete beams reinforced with CFRP laminates"*. (mathesis). Universitat Politècnica de Catalunya, 2011.

[6] H.-C. Wu and C. D. Eamon, (2017) *"Strengthening of concrete structures using fiber reinforced polymers (FRP): design, construction and practical applications"*:

[7] A. A. Yee and P. Eng, (2001) *"Structural and economic benefits of precast/prestressed concrete construction"* **PCI journal *46***(4): 34–43.

[8] R. Al-Rousan, M. Issa, and H. Shabila, (2012) *"Performance of reinforced concrete slabs strengthened with different types and configurations of CFRP"* **Composites Part B: Engineering *43***(2): 510–521. DOI: https://doi.org/10.1016/j.compositesb.2011.08.050.

[9] J. G. Teng, J. F. Chen, S. T. Smith, and L. Lam, (2003) *"Behaviour and strength of FRP-strengthened RC structures: a state-of-the-art review"* **Proceedings of the institution of civil engineers-structures and buildings *156***(1): 51–62. DOI: https://doi.org/10.1680/stbu.2003.156.1.51.

[10] P. O. Awoyera, F. Althoey, A. Bahrami, P. U. Apuye, B. S. Alotaibi, M. A. Abuhussain, et al., (2024) *"Structural retrofitting of RC slabs using bamboo fibre laminate: Flexural performance and crack patterns"* **Heliyon *10***(2): DOI: https://doi.org/10.1016/j.heliyon.2024.e23999.

[11] A. S. Azevedo, J. P. Firmo, J. R. Correia, R. M. Firouz, and J. A. Barros, (2023) *"Fire behaviour of reinforced concrete slab strips strengthened with prestressed NSM-CFRP laminates"* **Engineering Structures *297***: 116982. DOI: https://doi.org/10.1016/j.engstruct.2023.116982.

[12] M. Naser, R. Hawileh, and J. Abdalla, (2019) *"Fiber-reinforced polymer composites in strengthening reinforced concrete structures: A critical review"* **Engineering Structures *198***: 109542. DOI: https://doi.org/10.1016/j.engstruct.2019.109542.

[13] W. Ibrahim, M. El-adawy, and G. Ghanem. "Behaviour of reinforced concrete slabs strengthened by concrete overlays". In: *Construction Materials and Structures*. IOS Press, 2014, 956–962. DOI: https://doi.org/10.3233/978-1-61499-466-4-956.

[14] P. Mongkhonsang, (2018) *"Carbon Fiber Reinforced Polymers (CFRP) for Strengthening of Reinforced Concrete Structure"*:

[15] T. Mohammadi, B. Wan, K. A. Harries, and M. E. Sweriduk, (2017) *"Bond behavior of FRP–concrete in presence of intermediate crack debonding failure"* **Journal of Composites for Construction *21***(5): 04017018. DOI: https://doi.org/10.1061/(ASCE)CC.1943-5614.0000797.

[16] Y. M. Amran, R. Alyousef, R. S. Rashid, H. Alabduljabbar, and C.-C. Hung. "Properties and applications of FRP in strengthening RC structures: A review". In: *Structures*. ***16***. Elsevier. 2018, 208–238. DOI: https://doi.org/10.1016/j.istruc.2018.09.008.

[17] K. S. Elliott. *Precast concrete structures*. Crc Press, 2019.

[18] A. Siddika, M. A. Al Mamun, R. Alyousef, and Y. M. Amran, (2019) *"Strengthening of reinforced concrete beams by using fiber-reinforced polymer composites: A review"* **Journal of Building Engineering *25***: 100798. DOI: https://doi.org/10.1016/j.jobe.2019.100798.

[19] S. May, O. Steinbock, H. Michler, and M. Curbach. "Precast slab structures made of carbon reinforced concrete". In: *Structures*. ***18***. Elsevier. 2019, 20–27. DOI: https://doi.org/10.1016/j.istruc.2018.11.005.

[20] W. Derkowski and M. Surma, (2016) *"Composite action of precast hollow core slabs with structural topping"* **Czasopismo Techniczne**:

[21] S. Swathy, R. Preetha, J. Ashok Kumar, et al., (2024) *"Strengthening of Polypropylene fiber reinforced flat slab using BFRP fan and laminate against line loading."* **Procedia Structural Integrity *60***: 591–603. DOI: https://doi.org/10.1016/j.prostr.2024.05.079.

[22] A. ASTM, (2019) *"C39/c39m-18 standard test method for compressive strength of cylindrical concrete specimens. 2018"* **ASTM International: West Conshohocken, PA**:

[23] A. Standard, (2021) *"A421; Standard Specification for Stress-Relieved Steel Wire for Prestressed Concrete"* **ASTM International: West Conshohocken, PA, USA**:

[24] R. J. A. Syril and D. Rajkumar, *"Experimental Investigation of Ferrogeopolymer Confinement for Enhancing Brick Masonry Column Resilience under Axial Compression"*:

[25] A. ASTM, (2020) *"615/A 615M (2008),"Standard Specification for Deformed and Plain Carbon-Steel Bars for Concrete Reinforcement""* **ASTM International *100***: 19428–2959.

[26] A. Standard, (2018) *"ASTM A370-18: Standard Test Methods and Definitions for Mechanical Testing of Steel Products"*:

[27] V. H. Hoang, T. A. Do, A. T. Tran, and X. H. Nguyen, (2024) *"Flexural capacity of reinforced concrete slabs retrofitted with ultra-high-performance concrete and fiber-reinforced polymer"* **Innovative Infrastructure Solutions *9***(4): 113. DOI: https://doi.org/10.1007/s41062-024-01410-y.

[28] B. El-taly, Y. HasabElnaby, and N. Meleika, (2018) *"Structural performance of precast–prestressed hollow core slabs subjected to negative bending moments"* **Asian Journal of Civil Engineering *19***(6): 725–740. DOI: https://doi.org/10.1007/s42107-018-0061-0.

[29] M. A. Aiello, L. Ascione, A. Baratta, F. Bastianini, U. Battista, A. Benedetti, V. P. Berardi, A. Bilotta, A. Borri, B. Briccoli, et al., (2014) *"Guide for the design and construction of externally bonded FRP systems for strengthening existing structures"*: